SUPPLEMENTAL METHODS

Viral infections

Viral infections in tomato were performed as described in (1).

Quantitative PCR to measure viral accumulation

Quantitative PCR to determine viral accumulation was performed as described in (1), with primers to amplify *Rep*: TGAGAACGTCGTGTCTTCCG and TGACGTTGTACCACGCATCA (primer pair efficiency: 95%). 25S ribosomal DNA interspacer (ITS) was used as internal control (2).

Affinity-purification and mass spectrometry

Affinity-purification – mass spectrometry analysis (AP-MS) was performed as described in (3) with minor modifications. In order to efficiently extract membrane proteins, 2% of NP-40 was used in the protein extraction buffer.

Yeast two-hybrid screen

Yeast two-hybrid screening was performed by Hybrigenics Services, S.A.S., Paris, France (http://www.hybrigenics-services.com). The coding sequence of the C4 protein from *Tomato yellow leaf curl* virus (TYLCV) was PCR-amplified and cloned into pB27 as a C-terminal fusion to LexA DNA-binding domain (LexA-C4). The construct was checked by sequencing the entire insert and used as a bait to screen a random-primed TYLCV-infected tomato cDNA library constructed into pP6. pB27 and pP6 derive from the original pBTM116 (4) and pGADGH (5) plasmids, respectively. 109 million clones (more than 10-fold the complexity of the library) were screened using a mating approach with YHGX13 (Y187 *ade2-101*::*loxP-kanMX-loxP*, *mat*α) and L40ΔGal4 (*mat*a) yeast strains as previously described (6). 318 His+ colonies were selected on a medium lacking tryptophan, leucine and histidine. The prey fragments of the positive clones were amplified by PCR and sequenced at their 5' and 3' junctions. The resulting sequences were used to identify the corresponding interacting proteins in the GenBank database (NCBI) using a fully automated procedure.

Gel filtration assay

The C4 protein alone or co-expressed with the kinase domain of BAM1 ($BAM1_{674-1003}$), was purified by Ni-affinity column followed by anion exchange column. The purified proteins were subjected to a gel filtration assay (Superdex 200 Increase 10/300 GL column; GE Healthcare).

Northern blot of siRNA

Northern blots of siRNAs were performed as described in (7).

Root elongation assays

Root elongation assays with CLV3p were performed as described in (8).

Microprojectile bombardment assays

Microprojectile bombardment assays were performed as described (9). Four- to six-week-old expanded leaves of relevant Arabidopsis lines were bombarded with gold particles coated with pB7WG2.0.eGFP and pB7WG2.0.RFP_{ER} using a Bio-Rad Biolostic® PDS-1000/He Particle Delivery System. Bombardment sites were imaged 24 hours post-bombardment by epifluorescence (Leica DM6000) or confocal (Leica SP8) microscopy with a 25x water dipping lens and the number of cells to which GFP had spread was recorded (RFP_{ER} served as a marker to identify the transformed cell). For each line, data was collected from at least 3 independent bombardment events, each of which consisted of leaves from at least two individual plants. Statistical nonparametric Mann-Whitney analysis was performed using Genstat software.

In vitro kinase assay

The kinase domains of BAM1 or $BAM1_{D820N}$ (BAM1/$BAM1_{D820N\ 674-978}$) were expressed in *E. coli* and isolated by nickel-affinity column using buffer containing 50mM Tris-HCl pH 8.0, 200mM NaCl, 5mM β-mercaptoetanol. The protein was purified further by anion exchange and gel filtration chromatography. Radioactive in vitro kinase assays were performed as described in (10).

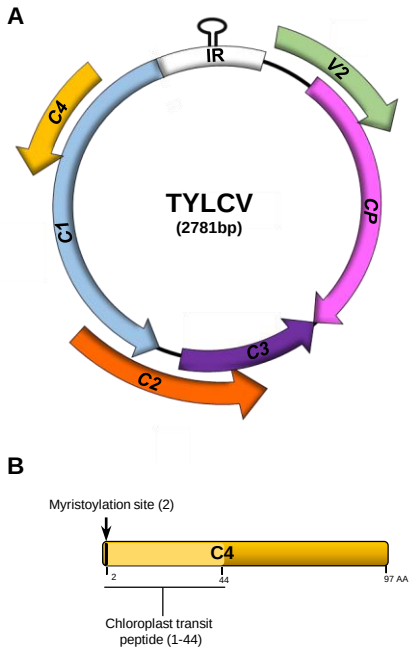

Figure S1. Genomic organization of *Tomato yellow leaf curl virus* (TYLCV) (A) and localization motifs in its C4 protein (B).

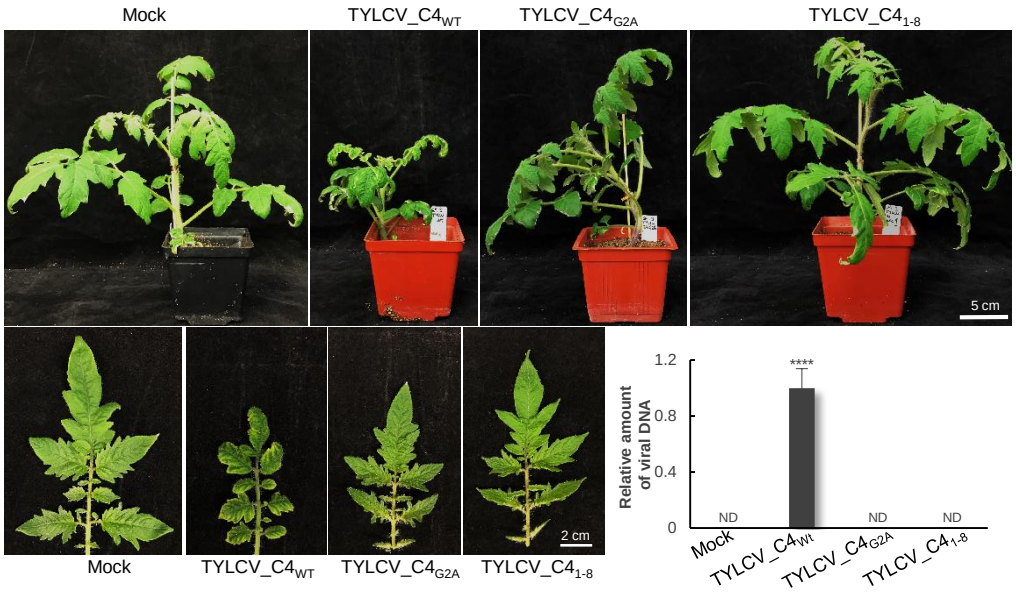

Figure S2. Tomato plants infected with TYLCV wild type, o mutant versions to express a non-myristoylable C4 (TYLCV_$C4_{G2A}$), or the first eight amino acids of C4 only (TYLCV_$C4_{1-8}$). The graph represents the relative viral DNA accumulation in plants inoculated with TYLCV variants or mock as determined by qPCR of total DNA extracted from apical leaves at 21 dpi. Values represent the average of 4 plants, and are relative to that of TYLCV_$C4_{WT}$. Error bars represent SE. Asterisks indicate a statistically significant difference (****, p-value < 0.0001), according to a Student's t-test; ND: not detectable.

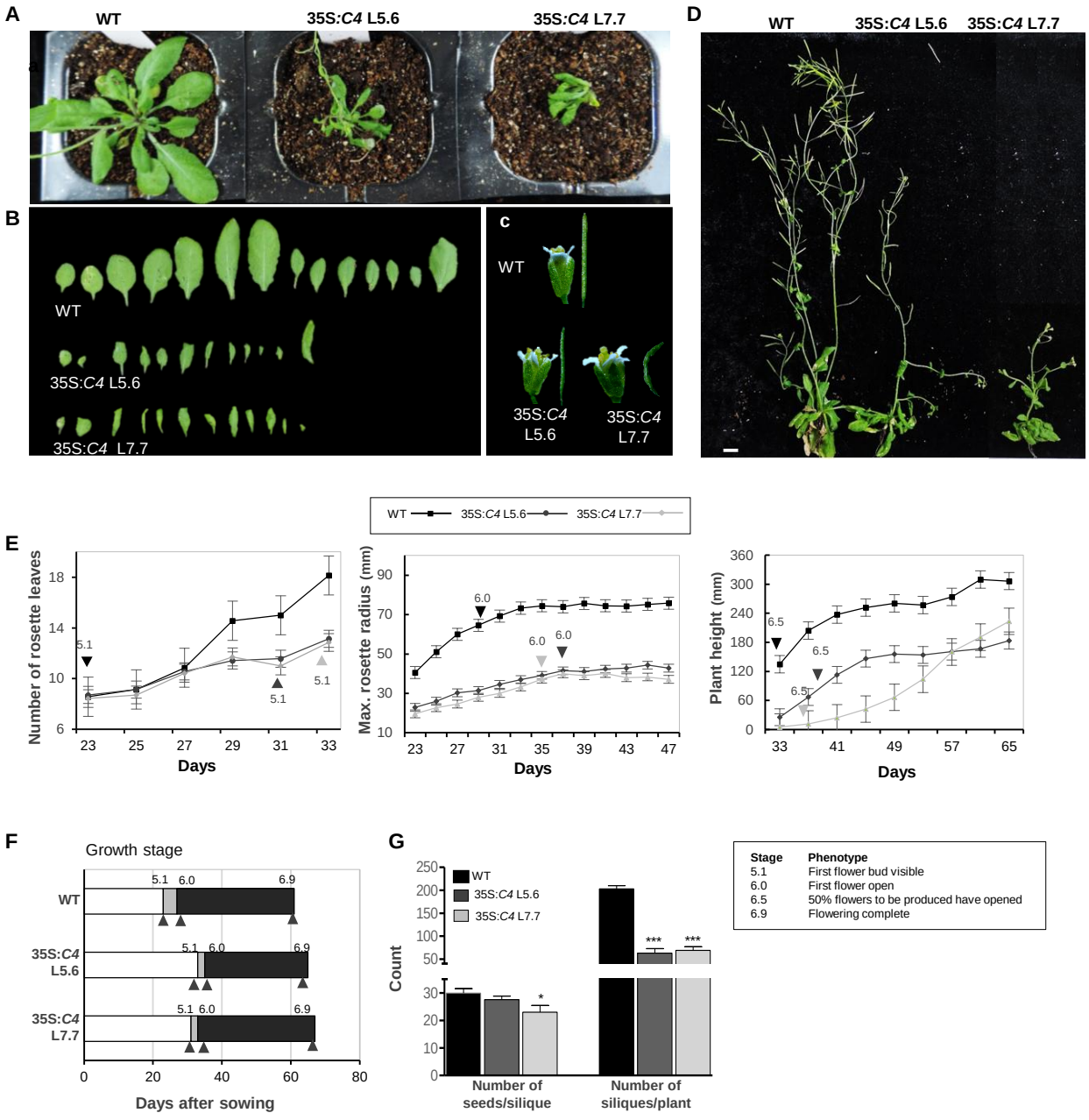

Figure S3. Developmental phenotypes of transgenic Arabidopsis plants expressing C4. A. Five-week-old transgenic plants grown in long day conditions. B. Leaves of five-week-old plants grown in long day conditions. C. Representative flowers and siliques. D. Flowering seven-week-old plants. E. Number of rosette leaves, maximum rosette radius, and plant height. Results are the average of ten plants. Error bars represent SE. F. Growth stage progression. Results are the average of ten plants. G. Numbers of seeds/silique and of siliques/plant. Results are the average of six plants.

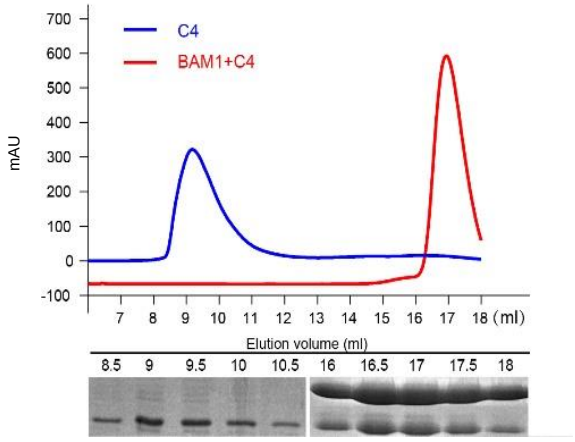

Figure S4. Gel filtration chromatography of C4 and the C4/BAM1 complex expressed in *Escherichia coli*. Top panel: gel filtration chromatograms of C4 and the C4/BAM1 complex. Bottom panel: Coomassie blue staining of the peak fractions shown above following SDS-PAGE. C4 eluted in the 8.5mL fraction on a Superdex 200 column, indicating aggregation, while both BAM1 and C4 eluted in the 16mL fraction after co-expression in *E.coli*. The peak shift of C4, combined with the co-migration of BAM1 and C4, shows that BAM1 can rescue C4 from aggregation by co-expression and directly binds C4.

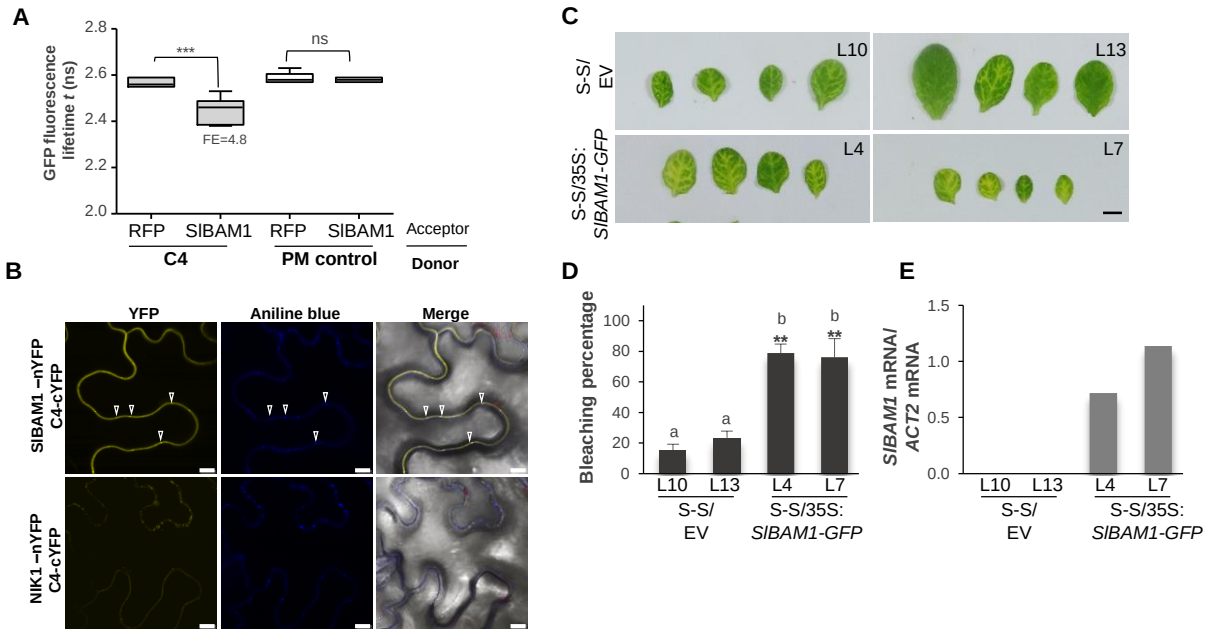

Figure S5. C4 interacts with BAM1 from tomato (SlBAM1). A. Interaction between C4 and SlBAM1 by FRET-FLIM upon transient co-infiltration in *N. benthamiana* leaves. The membrane protein NP_564431 (NCBI) is used as a negative control (PM control). FE: FRET efficiency. Asterisks indicate a statistically significant difference (***, p-value<0.005), according to a Student's t-test; ns: not significant. B. Interaction between C4 and SlBAM1 by BiFC upon transient co-infiltration in *N. benthamiana* leaves. The receptor-like kinase NIK1 is used as a negative control. Arrowheads indicate plasmodesmata. Scale bar: 10 µm. C. Leaves of four-week-old transgenic SUC:*SUL* plants overexpressing SlBAM1-GFP (S-S/35S:*SlBAM1-GFP*) or transformed with the empty vector (S-S/EV). Each set of leaves comes from one T2 plant from an independent line. D. Quantification of the bleaching percentage of the leaves in (C). Scale bar: 0.5 cm. Error bars represent SE; bars with the same letters are not significantly different (P=0.05) according to Dunnet's multiple comparison test. E. Expression of *SlBAM1* in transgenic S-S/35S:*SlBAM1-GFP* relative to actin mRNA, as measured by qPCR.

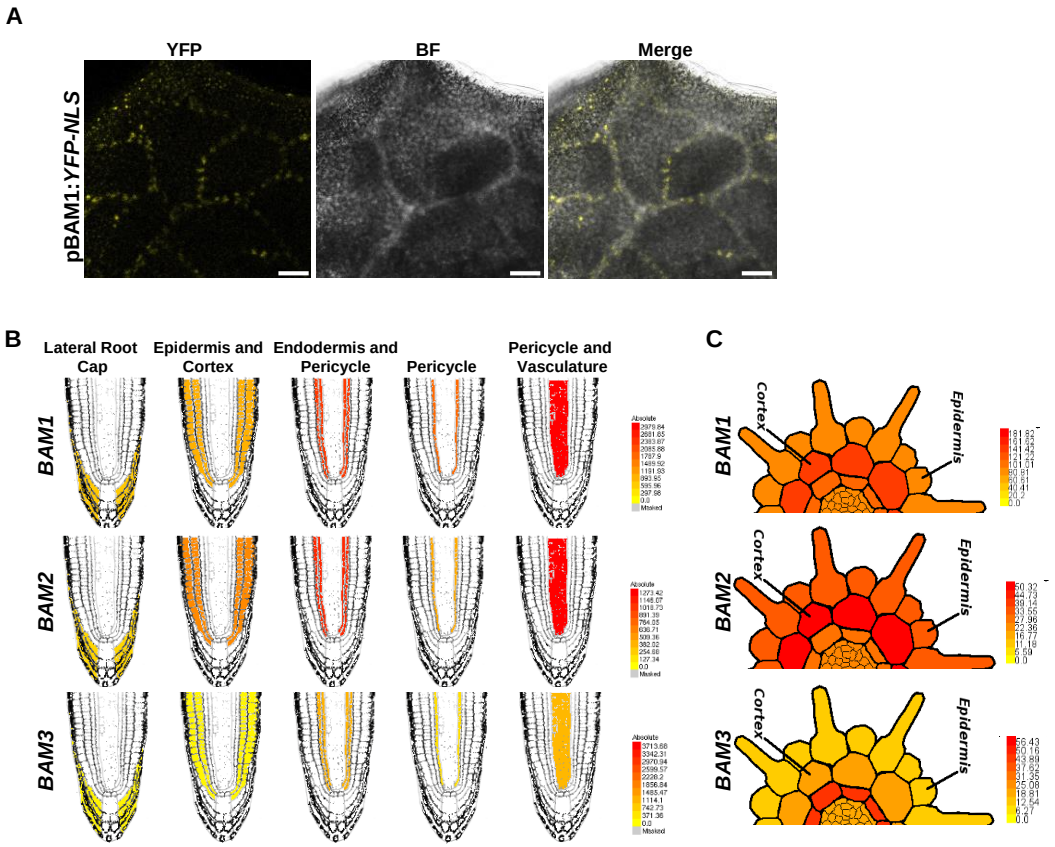

Figure S6. *BAM1* is strongly expressed in the vasculature, and its expression pattern overlaps with that of *BAM2* in roots. A. Leaves of twelve-day-old transgenic pBAM1:*YFP-NLS* Arabidopsis plants. BF: Bright field. Scale bar: 50 µm. B and C. Tissue-specific expression of *BAM1*, *BAM2*, and *BAM1* in roots (images taken from the Arabidopsis eFP browser, BAR (B; (11)), and Browser Express, from the Dinneny Lab (C; http://dinnenylab.dpb.carnegiescience.edu/browser/query); data in B are from (12); data in C are from (13)).

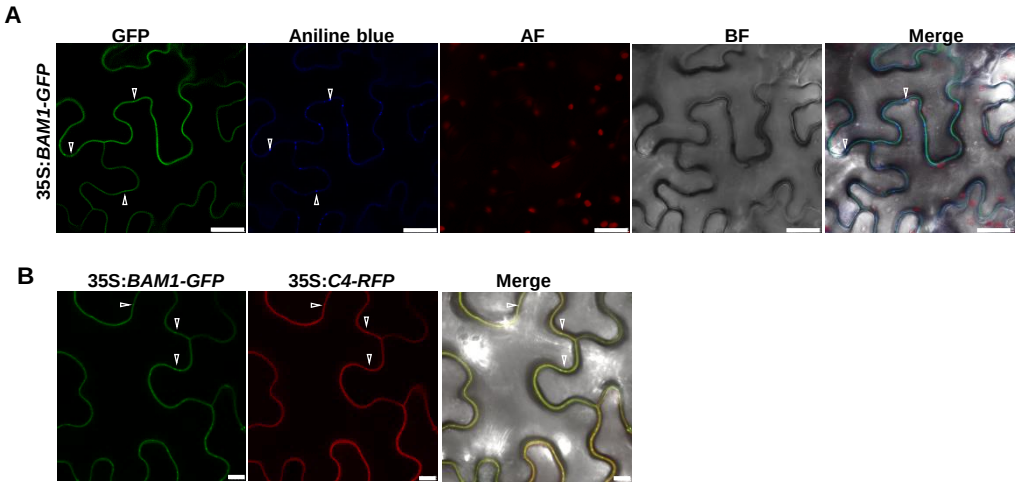

Figure S7. BAM1 co-localizes with C4 at plasma membrane and plasmodesmata. A. Subcellular localization of BAM1-GFP upon transient expression in *N. benthamiana* leaves. AF: Autofluorescence. BF: Bright field. Scale bar: 25 µm. B. Subcellular co-localization of BAM1-GFP and C4-RFP upon transient co-expression in *N. benthamiana* leaves. Arrowheads indicate plasmodesmata. Scale bar: 10 µm.

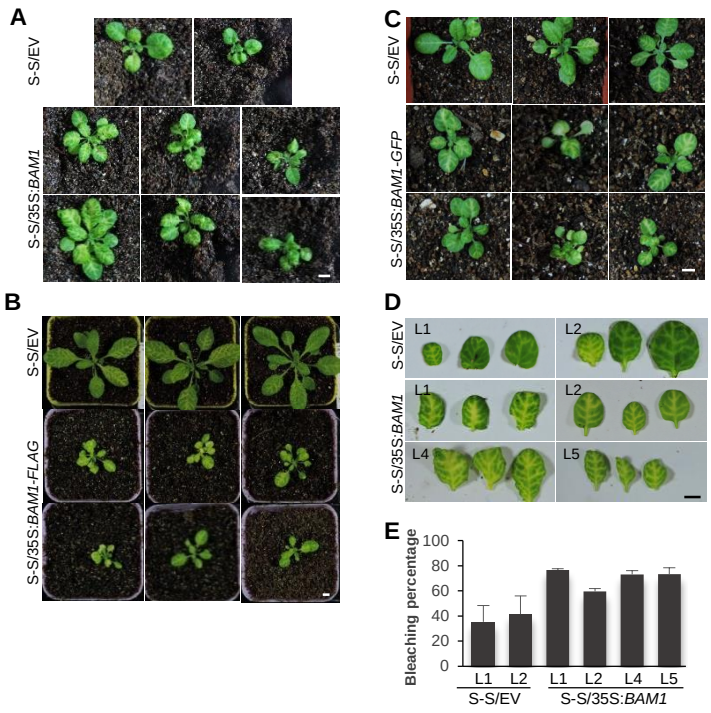

Figure S8. Phenotype of SUC:*SUL* plants overexpressing *BAM1*, *BAM1-GFP*, or *BAM1-FLAG*. A. Transgenic SUC:*SUL* lines overexpressing *BAM1* (S-S/35S:*BAM1*) or transformed with the empty vector (S-S/EV). B. Transgenic SUC:*SUL* lines overexpressing *BAM1-FLAG* (S-S/35S:*BAM1-FLAG*) or transformed with the empty vector (S-S/EV). C. Transgenic SUC:*SUL* lines overexpressing *BAM1-GFP* (S-S/35S:*BAM1-GFP*) or transformed with the empty vector (S-S/EV). D. Leaves of four-week-old transgenic SUC:*SUL* plants overexpressing *BAM1* (S-S/35S:*BAM1*) or transformed with the empty vector (S-S/EV). Each set of leaves comes from one T1 plant. E. Quantification of the bleaching percentage of the leaves in (D). Bars represent SE. Scale bar: 0.5 cm.

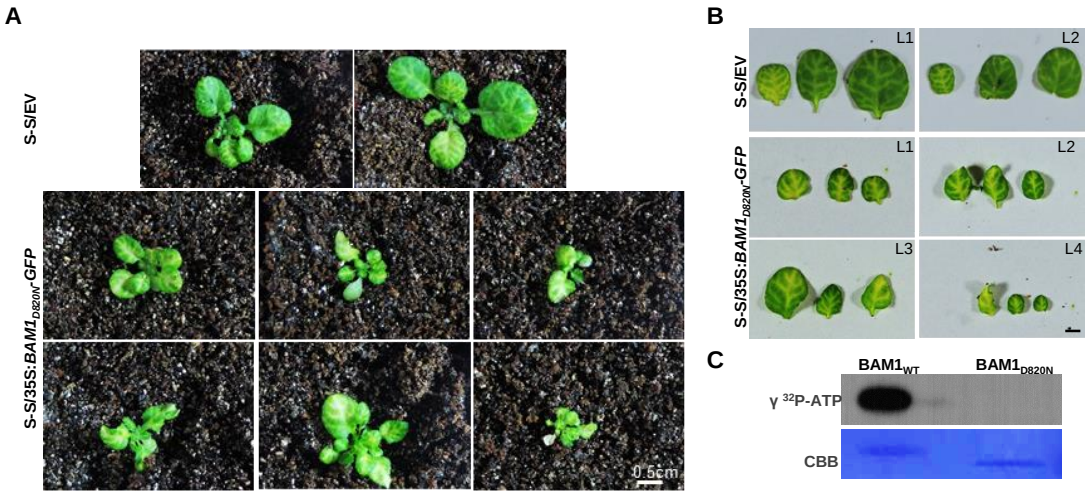

Figure S9. Phenotype of SUC:*SUL*/35S:*BAM1*$_{D820N}$-*GFP* lines. A. Four-week-old T1 plants grown in long-day conditions. B. Leaves of representative plants from (A). Scale bar: 0.5 cm. C. *In vitro* kinase assay with recombinant kinase domains from wild type BAM1 (BAM1$_{WT}$) and BAM1$_{D820N}$. The signal indicates autophosphorylation.

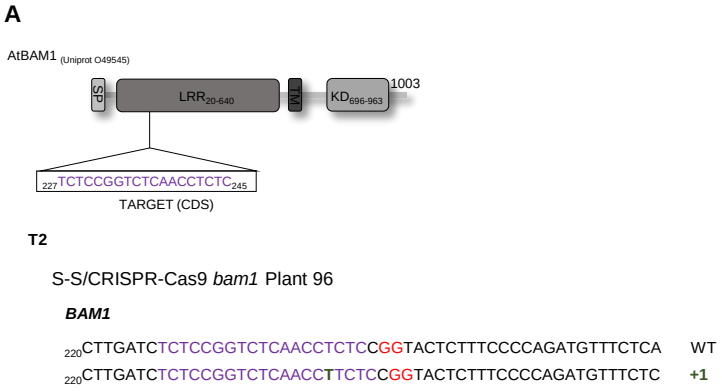

Figure S10. Details of the *bam1* mutations in the *bam1* single mutant generated by CRISPR-Cas9. The target of the CRISPR-Cas9 construct and the mutation in the plant depicted in Figure 3 are indicated (for details, see Supplementary table 1).

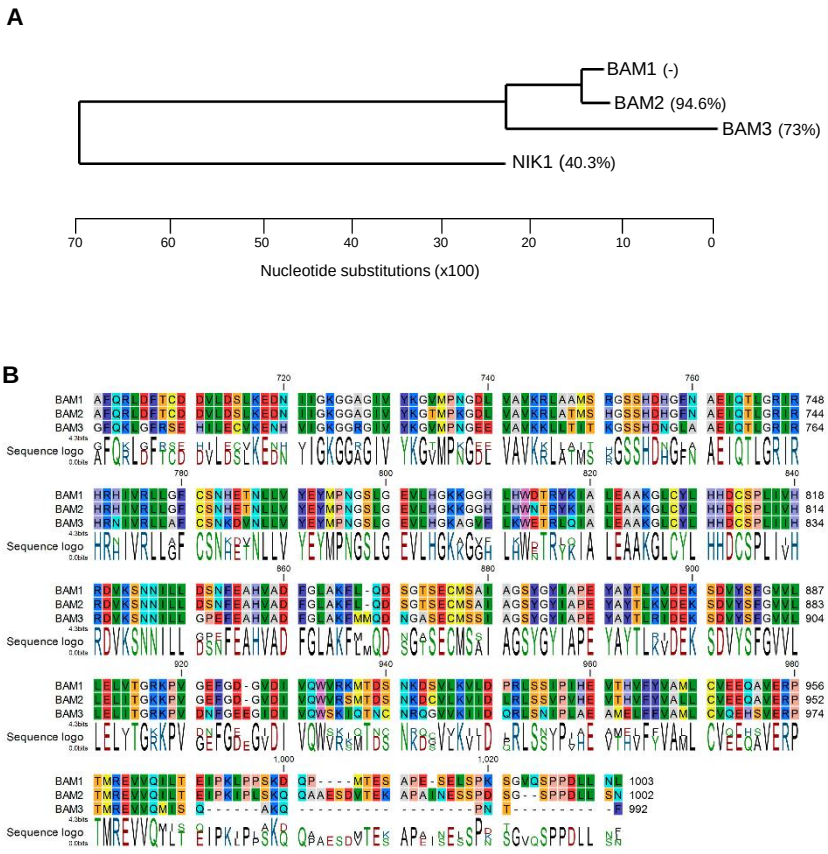

Figure S11. Phylogeny of the BAM1 family of receptor-like kinases. A. Phylogenetic tree of BAM1, BAM2, and BAM3, based on the kinase domain. The unrelated receptor-like kinase NIK1 is used as outgroup. Percentage of identity to BAM1 is indicated in parenthesis. B. Alignment of the kinase domain of BAM1, BAM2, and BAM3. The phylogenetic analysis and sequence alignment were performed using CLC Main Workbench 7.

A

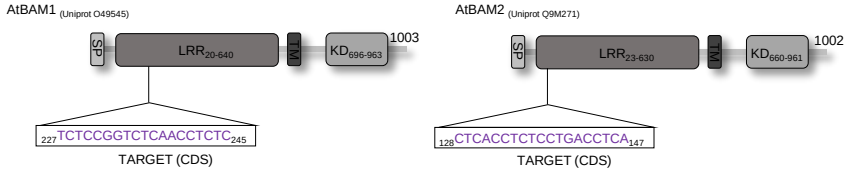

B

T3

L1.8 (Plant 4)

BAM1

220CTTGATCTCTCCGGTCTCAACCTCTCCGGTACTCTTTCCCCAGATGTTTCTCA WT

220CTTGATCTCTCCGGTCTCAACCTTCTCCGGTACTCTTTCCCCAGATGTTTCTC +1

220CTTGATCTCTCCGGTCTCAACCATCTCCGGTACTCTTTCCCCAGATGTTTCTCA +1

220CTTGATCTCTCCGGTCTCAACC . CTCCGGTACTCTTTCCCCAGATGTTTCTCA -1

220CTTGATCTCTCCGGTCTCAAC . . CTCCGGTACTCTTTCCCCAGATGTTTCTCA -2

BAM2

120CGACGAACACTCACCTCTCCTGACCTCATGGAACCTTTCAACAACTTTCTGTT WT

120CGACGAACACTCACCTCTCCTGACCCTCATGGAACCTTTCAACAACTTTCTGTT +1

L1.41 (Plant 24)

BAM1

220CTTGATCTCTCCGGTCTCAACCTCTCCGGTACTCTTTCCCCAGATGTTTCTCA WT

220CTTGATCTCTCCGGTCTCAAC . . CTCCGGTACTCTTTCCCCAGATGTTTCTCA -2

BAM2

120CGACGAACACTCACCTCTCCTGACCTCATGGAACCTTTCAACAACTTTCTGTT WT

120CGACGAACACTCACCTCTCCTGACCCTCATGGAACCTTTCAACAACTTTCTGTT +1

Figure S12. Details of the *bam1* and *bam2* mutations in the *bam1 bam2* double mutants generated by CRISPR-Cas9. The target of the CRISPR-Cas9 construct and the mutations in the plants depicted in Figure 4 are indicated (for details, see Supplementary table 1).

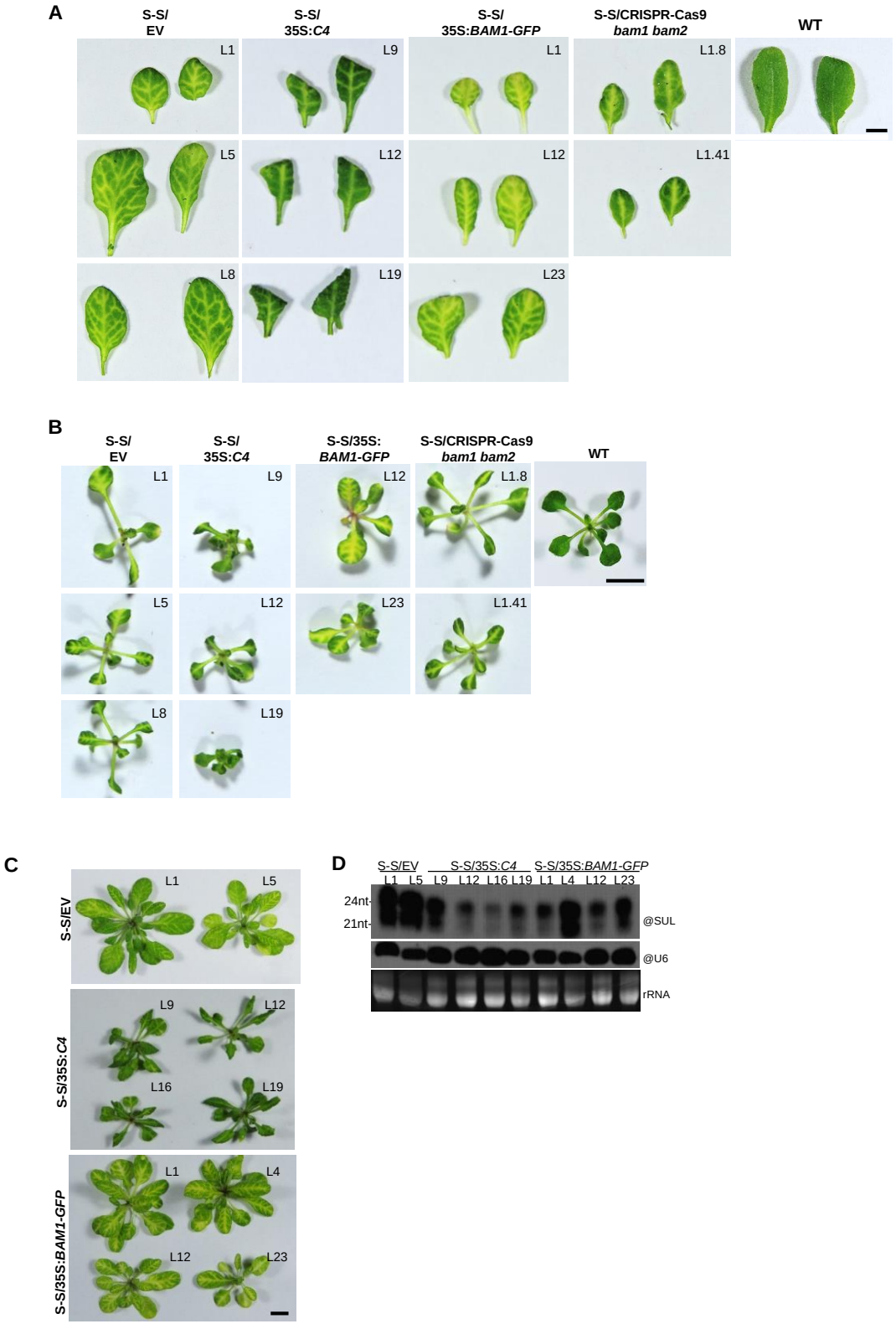

Figure S13. *SUL* silencing phenotype in SUC:*SUL* lines expressing *C4*, overexpressing *BAM1*, or mutated in *BAM1* and *BAM2*. A. Rosette leaves of four-week-old plants. These leaves were used for the qPCR experiments depicted in Figure 5A and B. B. Two-week-old seedlings. These seedlings were used for the sRNA sequencing depicted in Figure 5C. C. Four-week-old plants. Each plant comes from one T2 independent line. D. *SUL* siRNA accumulation in the plants depicted in C. Scale bar: 0.5 cm.

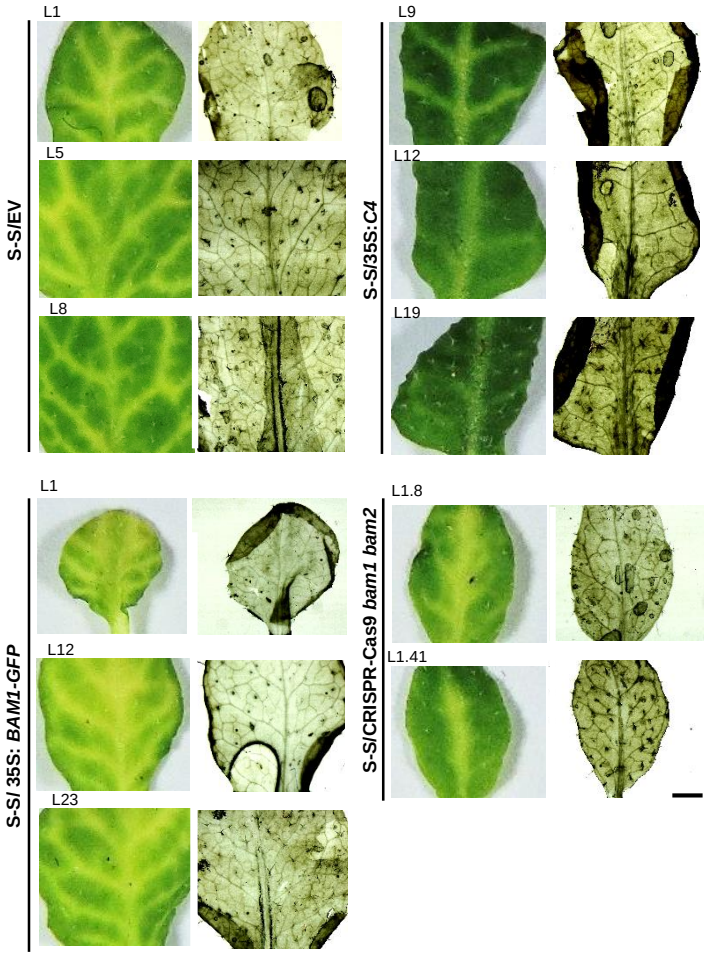

Figure S14. Spread of silencing and venation pattern in transgenic SUC:*SUL* plants expressing *C4*, overexpressing *BAM1*, mutated in *BAM1* and *BAM2*, or control (EV). Leaves are detached from four-week-old plants; each leaf comes from one independent line. Scale bar: 0.1 cm.

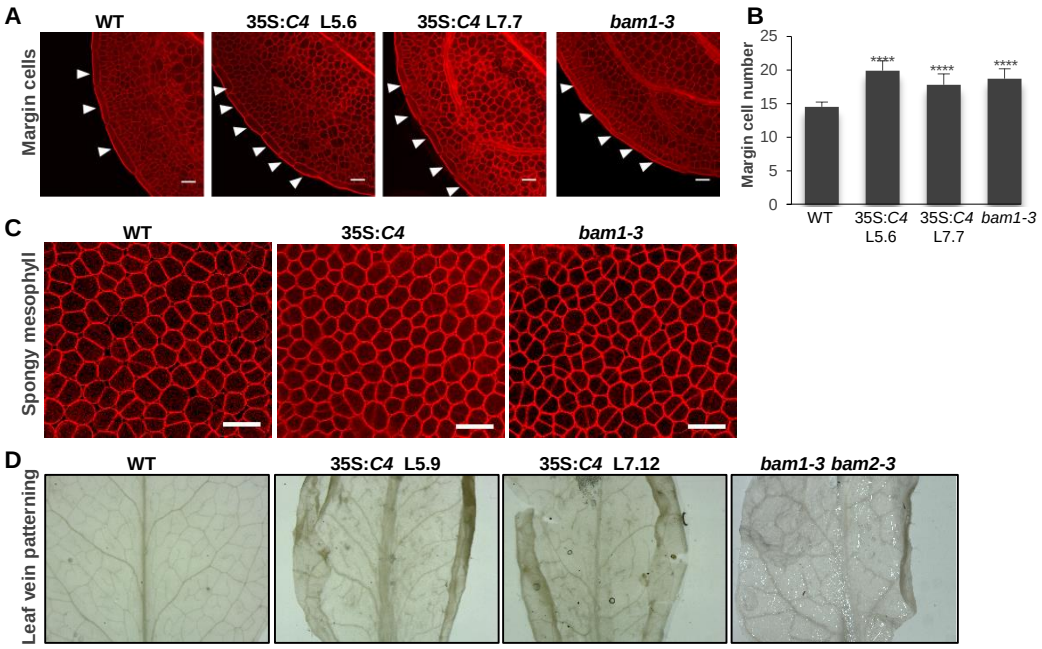

Figure S15. Similar developmental phenotypes in the transgenic Arabidopsis lines expressing *C4* and the *bam1-3* single or *bam1-3 bam2-3* double mutant. A. Margin cells in cotyledons of two-day-old seedlings. Scale bar: 25 µm. B. Margin cell numbers of cotyledons of two-day-old seedlings. Asterisks indicate a statistically significant difference (****, p-value <0.0001), according to a Student's t-test. C. Spongy mesophyll of cotyledons of two-day-old seedlings. Scale bar: 25 µm. D. Leaf vein patterning in leaves of five-week-old plants.

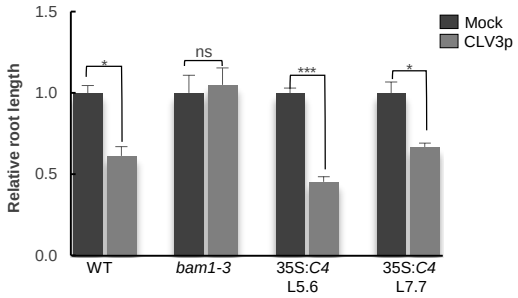

Figure S16. Root response to CLV3p in transgenic seedlings expressing *C4*. Wild-type (Col-0) and *bam1-3* mutant seedlings are used as control. Asterisks indicate a statistically significant difference (***,p-value < 0.005; *, p-value < 0.05), according to a Student's t-test; ns: not significant.

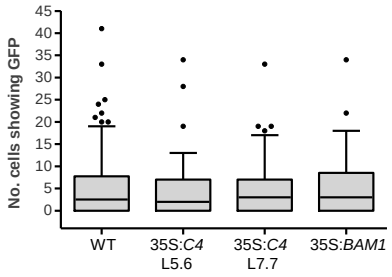

Figure S17. Plasmodesmal flux is not altered in lines expressing *C4* or overexpressing *BAM1*. Box plot of data from microprojectile bombardment assays. 35S:*GFP* diffused to the same number of cells in wild-type Col-0 and lines 35S:*C4* L5.6 (p-value 0.658), 35S:*C4* L7.7 (p-value 0.831), and 35S:*BAM1* (p-value 0.926). Boxes indicate the interquartile range with the line indicating the median value; whiskers are 1.5 time the interquartile range.

Table S1. Mutations in *BAM1* and *BAM2* obtained by CRISPR-Cas9.

Gene	Edition number	Nucleotides			Protein		Sequence (TARGET, PAM)
		Target	Change	Position	Change	Size AA	
BAM1							
	WT	-	-	-	-	1003	$_{220}$CTTGATCTCTCCGGTCTCAACC-TCTCCGGTACTCTT$_{255}$
	1	227-245	+1	$_{241}$T$_{242}$	Stop	101	$_{220}$CTTGATCTCTCCGGTCTCAACCTTCTCCGGTACTCTT$_{256}$
	2	227-245	+1	$_{241}$A$_{242}$	Stop	101	$_{220}$CTTGATCTCTCCGGTCTCAACCATCTCCGGTACTCTT$_{256}$
	3	227-245	-1	T$_{242}$	Stop	103	$_{220}$CTTGATCTCTCCGGTCTCAACC--CTCCGGTACTCTT$_{254}$
	4	227-245	-2	CT$_{241-242}$	Stop	100	$_{220}$CTTGATCTCTCCGGTCTCAACC---TCCGGTACTCTT$_{253}$
BAM2							
	WT	-	-	-	-	1002	$_{120}$CGACGAACACTCACCTCTCCTGACC-TCATGGAACCTT$_{156}$
	1	129-147	+1	$_{144}$C$_{145}$	Stop	79	$_{120}$CGACGAACACTCACCTCTCCTGACCCTCATGGAACCTT$_{157}$

Gene	Generation	Number	Editions	
			BAM1	***BAM2***
BAM1				
	T2	Plant 96	Edition 1-/-	WT
	T3	L1.8 (Plant 4)	Edition 1, Edition 2, Edition 3, Edition 4	Edition 1-/-
	T3	L1.41 (Plant 24)	Edition 4-/-	Edition 1-/-

Table S2. Plasmids generated in this work.

Plasmid name/ Gene identifier	Vector Entry	Vector backbone/ template	Primers to clone in entry vectors
TOPO-*C4*-S (with stop codon)	pENTRD/TOPO (Invitrogen)		F: CACCATGGGAACCACATC R: TTAATATATTGAGGG
TOPO-*C4*-NS (without stop codon)	pENTRD/TOPO (Invitrogen)		F: CACCATGGGAACCACATC R: ATATATTGAGGGCCTC
TOPO-$C4_{G2A}$-NS (without stop codon)	pENTRD/TOPO (Invitrogen)		F:CACCATGGCGAACCACATCTCCAT R: TTAATATATTGAGGGCCTCGG
pET21b-*C4*	pET21b (Novagen)	TOPO-*C4*-S	F: AAAACCTCTACTTCCAATCGATGGGGAACCACATCTCCATG R: CCACACTCATCCTCCGGTTAATATATTGAGGGCCTCGG
TOPO-*AtBAM1*-S (with stop codon)/At5g65700	pENTRD/TOPO (Invitrogen)		F: CACCATGAAACTTTTTCTTCTCCT R: TCATAGATTGAGTAGATCCGG
TOPO-*AtBAM1*-NS (without stop codon)	pENTRD/TOPO (Invitrogen)		F: CACCATGAAACTTTTTCTTCTCCT R: TAGATTGAGTAGATCCGG
pET21-*AtBAM1-KD* (678-1003aa)	pET21b (Novagen)	TOPO-*AtBAM1*-S	F: AAAACCTCTACTTCCAATCGACAGCTTTCCAGAGACTAGAC R: CCACACTCATCCTCCGGTCATAGATTGAGTAGATCCGG
pET21-*AtBAM1-KD* (678-974 aa)	pET21b (Novagen)	TOPO-*AtBAM1*-S	F: AAAACCTCTACTTCCAATCGACAGCTTTCCAGAGACTAGAC R: CCACACTCATCCTCCGGTGGCAACTTCGGGATCTCAGT
TOPO-$AtBAM1_{D820N}$-NS (without stop codon)		Mutagenesis in TOPO-*AtBAM1*-NS	F:CCATTGATCGTTCACAGAAATGTCAAA TCAAACAACATC R:GGTAACTAGCAAGTGTCTTTACAGTTT AGTTTGTTGTAG
pET21-$AtBAM1\text{-}KD_{D820N(678\text{-}974\ aa)}$	pET21b (Novagen)	TOPO-$AtBAM1_{D820N}$-NS	F: AAAACCTCTACTTCCAATCGACAGCTTTCCAGAGACTAGAC R: CCACACTCATCCTCCGGTGGCAACTTCGGGATCTCAGT
TOPO-*AtBAM2*-NS (without stop codon)/At3g49670			F: CACCATGAAGCTTCTTCTTC R: ATTACTTAAAAGATCCGGTG
TOPO-*AtBAM3*-NS (without stop codon)/At4g20270			F:CACCATGGCAGACAAGATCTTCAC R:GAAAGTATTAGGCTGTTTAGCCTGAG
TOPO-*SlBAM1*-NS (without stop codon)/ Solyc02g091840.2.1			F:CACCATGCGTCTTCTTTTTTTTCTTC R:GATACTGAGTAGGTCAGGTGGAGG
TOPO-*AtNIK1*-NS (without stop codon)/At5g16000			F:CACCATGGAGAGTACTATTG R:TCTAGGACCAGAGAGCTCCA
pDONR-pBAM1	pDONR/Zeo (Invitrogen)		F:GGGGACAAGTTTGTACAAAAAAGCAGGCTCA ATGATCCGATCCTCAAAAGTATGTA R:GGGGACCACTTTGTACAAGAAAGCTGGGTC TGTTTCTCTCTATCTCTCTTGTGTG
TOPO-TYLCV			1.4 copies of TYLCV genome. Synthetized starting at 2334 nt
TOPO-TYLCV_$C4_{G2A}$		Mutagenesis in TOPO-TYLCV	F: GGAGATGTGGTTCGCCATTCTCGTGG AGTTC R: GAACTCCACGAGAATGGCGAACCACATCTCC
TOPO-TYLCV_$C4_{1\text{-}8}$		Mutagenesis in TOPO-TYLCV	F:GCCTTCGAATTGGATTAGCACATGGAGATGTGG R:CCACATCTCCATGTGCTAATCCAATTCGAAGGC
35S:*C4*	TOPO-*C4*-S	pGWB2	

35S:*$C4_{G2A}$*	TOPO-*$C4_{G2A}$*-NS	pGWB505	
35S:*C4-GFP*	TOPO-*C4*-NS	pGWB5	
35S:*C4-3xHA*	TOPO-*C4*-NS	pGWB514	
35S:*C4-RFP*	TOPO-*C4*-NS	pB7RWG2.0	
35S:*BAM1*	TOPO-*AtBAM1*-S	pGWB2	
35S:*BAM1-GFP*	TOPO-*AtBAM1*-NS	pGWB505	
35S:*BAM1-FLAG*	TOPO-*AtBAM1*-NS	pGWB511	
35S:BAM1-RFP	TOPO-*AtBAM1*-NS	pB7RWG2.0	
35S:*$BAM1_{D820N}$-GFP*	TOPO-*$AtBAM1_{D820N}$*-NS	pGWB505	
35S:*BAM2-GFP*	TOPO-*AtBAM2*-NS	pGWB505	
35S:*BAM3-GFP*	TOPO-*AtBAM2*-NS	pGWB505	
35S:*NIK1-GFP*	TOPO-*AtNIK1*-NS	pGWB505	
35S:*SlBAM1-GFP*	TOPO-*SlBAM1*-NS	pGWB505	
C4-cYFP	TOPO-*C4*-NS	pGTQL1221YC	
BAM1-nYFP	TOPO-*AtBAM1*-NS	pGTQL1211YN	
BAM2-nYFP	TOPO-*AtBAM2*-NS	pGTQL1211YN	
BAM3-nYFP	TOPO-*AtBAM3*-NS	pGTQL1211YN	
NIK1-nYFP	TOPO-*AtNIK1*-NS	pGTQL1211YN	
SlBAM1-nYFP	TOPO-*SlBAM1*-NS	pGTQL1211YN	
RFP		pGBWB555	
pBAM1:YFP-NLS	pDNOR-pBAM1	pBGYN	
TYLCV infectious clone	TOPO-TYLCV	pGWB501	
TYLCV	TOPO-TYLCV	pGWB501	
TYLCV_$C4_{G2A}$	TOPO-TYLCV_$C4_{G2A}$	pGWB501	
TYLCV_$C4_{1-8}$	TOPO-TYLCV_$C4_{1-8}$	pGWB501	
BAM-sgRNA		pCAMBIA1300	BAM1-sgF GATTGTCTCCGGTCTCAACCTCTC
			BAM1-sgR AAACGAGAGGTTGAGACCGGAGAC
			BAM2-sgF GGTCGCTCACCTCTCCTGACCTCA
			BAM2-sgR AAACTGAGGTCAGGAGAGGTGAGC

SUPPLEMENTAL REFERENCES

1. Lozano-Duran R, Rosas-Diaz T, Luna AP, & Bejarano ER (2011) Identification of host genes involved in geminivirus infection using a reverse genetics approach. *PloS one* 6(7):e22383.
2. G. Mason, P. Caciagli, G. P. Accotto, E. Noris, Real-time PCR for the quantitation of Tomato yellow leaf curl Sardinia virus in tomato plants and in Bemisia tabaci. *Journal of virological methods* **147**, 282-289 (2008).
3. Y. Sang, Y. Wang, H. Ni, A. C. Cazalé, Y. M. She, N. Peeters, A. P. Macho, The Ralstonia solanacearum type III effector RipAY targets plant redox regulators to suppress immune responses. *Molecular Plant Pathology* doi:10.1111/mpp.12504 (2016).
4. Vojtek AB & Hollenberg SM (1995) Ras-Raf interaction: two-hybrid analysis. *Methods in enzymology* 255:331-342.
5. Bartel P, Chien CT, Sternglanz R, & Fields S (1993) Elimination of false positives that arise in using the two-hybrid system. *BioTechniques* 14(6):920-924.
6. Fromont-Racine M, Rain JC, & Legrain P (1997) Toward a functional analysis of the yeast genome through exhaustive two-hybrid screens. *Nature genetics* 16(3):277-282.
7. Yang DL, et al. (2016) Dicer-independent RNA-directed DNA methylation in Arabidopsis. Cell research 26(11):1264.
8. Shimizu N*, et al.* (2015) BAM 1 and RECEPTOR-LIKE PROTEIN KINASE 2 constitute a signaling pathway and modulate CLE peptide-triggered growth inhibition in Arabidopsis root. *The New phytologist* 208(4):1104-1113.
9. Thomas CL, Bayer EM, Ritzenthaler C, Fernandez-Calvino L, & Maule AJ (2008) Specific targeting of a plasmodesmal protein affecting cell-to-cell communication. PLoS biology 6(1):e7.
10. Macho AP *et al*., (2014). A bacterial tyrosine phosphatase inhibitis plant pattern recognition receptor activation. Science 343(6178):1509-12.
11. Winter D, Vinegar B, Nahal H, Ammar R, Wilson GV, Provart NJ (2007). An “Electronic Fluorescent Pictograph” browser for exploring and analysing large-scale biological data sets. *PLoS One* 8;2(6):e718.

12. Gifford ML, Dean A, Gutierrez RA, Coruzzi GM, Birnbaum KD (2008). Cell-specific nitrogen response mediate developmental plasticity. *Proc Natl Acad Sci U S A* 15;105(2):803-8.

13. Geng Y, Wu R, Wee CX, Xie F, Wei X, Chan PM, Tham C, Duan L, Dinneny JR (2013). A spatio-temporal understanding of growth regulation during the salt stress response in Arabidopsis. *Plant Cell* 25(6):2132-54.